by EFLS and other techniques.

Jennings[2] had alluded to a disadvantage of EFLS; namely, that the polymer size must be comparable to the wavelength of light. This can be overcome by using low-angle X-ray (LAXS) and neutron scattering (LANS) techniques in the presence of an electric field. The theory presented here would apply in the case of LAXS and LANS in an electric field, except that the polarizability α would be replaced by electron density and scattering length, respectively.

Conclusions

Electric field induced light scattering is a technique that is potentially useful in several areas of polymer characterization. By doing two EFLS experiments on the same polymer sample, one can separate out the two effects contributing to EFLS, namely, the fluctuation term which comes about from polymer flexibility and the orientation term. The first term is important for determining the degree of polymer flexibility and is useful for characterizing liquid-crystal polymers. For example, it can be used to distinguish between rods, disks, and semiflexible polymers. The second term will be sensitive to the details of polymer structure and can complement other methods for characterizing polymer, such as end-to-end distances, dipole moments, and Kerr effect. When EFLS is performed in the small-angle scattering regime, the theoretical expression for it can be evaluated exactly by using the RIS model.[9] In that case, there can be a simple direct comparison between experiment and theory.

References and Notes

(1) Berne, B. J.; Pecora, R. *Dynamic Light Scattering*; Wiley: New York, 1976; Chapters 7 and 8.
(2) Jennings, B. R. In *Molecular Electrooptics*; C. T., O'Konski, Ed.; Marcel Dekker: New York, 1978; Vol. 1, p 275.
(3) Khanarian, G.; Tonelli, A. E. In *Nonlinear Optical Properties of Organic and Polymeric Materials*; Williams, D. J., Ed.; ACS Symposium Series 233; American Chemical Society: Washington, DC, 1983; p 235.
(4) Khanarian, G. *Macromolecules* **1982**, *15*, 1429.
(5) Wippler, C.; Benoit, H. *Makromol. Chem.* **1954**, *13*, 7.
(6) Wallach, M. L.; Benoit, H. *J. Polym. Sci. Polym. Phys. Ed.* **1966** *4*, 491.
(7) Bottcher, C. J. F. *Theory of Electric Polarization*; revised by van Belle, O. C., Boredewijk, P., Rip, A.; Elsevier: Amsterdam, 1973; Vol. 1, Chapter 5.
(8) Edmunds, A. R. *Angular Momentum in Quantum Mechanics*; Princeton University Press: Princeton, NJ, 1957; Chapters 3, 4, 5.
(9) Flory, P. J. *Statistical Mechanics of Chain Molecules*; Interscience, New York, 1969.
(10) See articles in: *Recent Advances in Liquid Crystal Polymers*; Chapoy, L. L., Ed.; Elsevier: Amsterdam, 1985.

Dynamic Light Scattering Studies of Polymer Solutions. 6. Polyisoprenes in a Θ-Solvent, 1,4-Dioxane

Yoshisuke Tsunashima,* Masukazu Hirata, Norio Nemoto, Kanji Kajiwara, and Michio Kurata

Institute for Chemical Research, Kyoto University, Uji, Kyoto-fu 611, Japan.

Received May 13, 1987

ABSTRACT: The dynamic properties of polyisoprenes in 1,4-dioxane at 34.7 °C (the Θ-temperature) have been studied by homodyne photon correlation spectroscopy. The infinite dilution characteristics, the translational diffusion coefficient D_0, and the effective decay rate (the first cumulant) $(\Gamma_e)_{c\to 0}$, have been analyzed as functions of the scattering vector q. It has been found that isoprene chains in the unperturbed state are fairly well described by the *nondraining* Gaussian model with *nonpreaveraged* Oseen hydrodynamic interaction. However, it has been revealed that some 10% and some 20% differences of D_0 and $(\Gamma_e)_{c\to 0}$, respectively, exist between experiments and theories. The former difference might be explainable in terms of the *internal friction* of chains, which has recently been introduced by Fixman. The concentration dependence of the translational diffusion coefficient is also discussed in some detail.

Introduction

At the Θ-temperature where the excluded volume effect vanishes, dynamic light scattering by dilute polymer solutions provides precise information on the nature of the hydrodynamic interaction between chain segments. Experimental studies[1-3] so far made for an oridinary Θ-solution, polystyrene (PS) in cyclohexane, *trans*-decalin, and so on, have shown some puzzling results, for example, the superiority of the preaveraged (PA) form of the Oseen hydrodynamic interaction to the non-PA form and a 15% or 20% reduction of the translational diffusion coefficient D_0 from the Kirkwood value. These situations have been clearly summarized in the recent review of Stockmayer and Hammouda.[4] Similar results, though not very conclusive, have been obtained also for PS in benzene, a good solvent.[5]

We have recently studied[6] the dynamic behavior of polyisoprene (PIP) in cyclohexane and found that, in the good solvent, PIP chains are well described by the non-draining chain model with the non-PA Oseen tensor and with Domb-Gillis-Wilmers segment distribution. This result which is more reasonable as compared with the previous result for PS seems to be attributed to higher

Table I
Characteristics of Polyisoprenes in 1,4-Dioxane at 34.7 °C (Θ-Temperature)

polymer	$10^{-6}M_w$[a]	R_G, 10^{-6} cm	microstructure[b] cis-1,4	trans-1,4	3,4
L-14	0.326	(1.91)[c]	73.3	21.9	4.8
L-12	0.568	2.53	67.0	25.3	7.7
L-11	2.44	(5.23)	84.1	11.9	4.0

[a] Measured in cyclohexane at 25 °C.[6] [b] Measured in $CDCl_3$ at 35 °C by using a 400-MHz ^1H NMR spectrometer.[6] [c] The values in parentheses were estimated from the empirical relation $R_G = 3.35 \times 10^{-9}M_w^{0.50}$ cm, which was obtained by analyzing the data of Hadjichristidis and Roovers[7] and ours.

0024-9297/87/2220-2862$01.50/0 © 1987 American Chemical Society

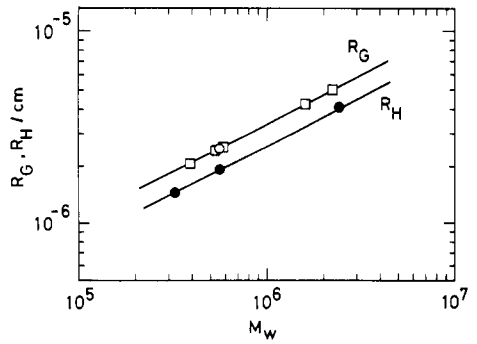

Figure 1. Logarithmic plots of the equivalent hydrodynamic radius R_H and the root-mean-square radius of gyration R_G against the weight-average molecular weight M_w for PIP in 1,4-dioxane at the Θ-temperature: circles represent the present data at 34.7 °C; squares the data of Hadjichristidis and Roovers at 34 °C.[7]

chain flexibility of PIP chains.

Thus, in this paper, we reexamine experimentally the dynamic behavior of the unperturbed chain by using another Θ-solution, PIP, in 1,4-dioxane at 34.7 °C.

Experimental Section

Materials. Three samples, coded as L-14, L-12, and L-11, of previously investigated PIPs[6] were used in this study. Their molecular weights ranged from 0.326×10^6 to 2.44×10^6. The homogeneity was verified[6] by the value $M_w/M_n < 1.1$. The characteristics of these samples are summarized in Table I. The root-mean-square radius of gyration of the polymer (R_G) in 1,4-dioxane at 34.7 °C was measured only for L-12 in the present work. This value, 2.53×10^{-6} cm, agreed with the data of Hadjichristidis and Roovers[7] as shown in Figure 1. Here an unfilled circle represents our value for L-12 and five squares represent Hadjichristidis and Roovers data at 34 °C. Their samples had the microstructure similar to ours; 70% cis-1,4, 23% trans-1,4, and 7% 3,4. All these data are well fitted by a straight line:

$$R_G = 3.35 \times 10^{-9} M_w^{0.50\pm0.01} \quad \text{(cm)} \qquad (1)$$

We estimated R_G of the remaining two samples, L-14 and L-11, by using eq 1. These values are shown in parentheses in Table I.

1,4-Dioxane (spectrograde, Nakarai Chemicals, Kyoto) was used without further purification. Its purity was checked by measuring the refractive index n for the sodium D line at 25 °C in a Pulfrich refractometer (Shimadzu Seisakusho Co., Kyoto). The result was that $n^{25}_D = 1.4199$, which agreed well with the literature value, 1.42025.[8] We also estimated the refractive index, the density, and the viscosity of 1,4-dioxane at 34.7 °C (Θ-temperature[9]) as n = 1.4197 (488 nm) and 1.4137 (633 nm), $d = 1.0167$ g cm^{-3}, and $\eta_0 = 1.019 \times 10^{-2}$ g cm^{-1} s^{-1}, respectively, by using the literature values. A bottle containing the solvent was filled with fresh N_2 every time immediately after use and was stored in a desiccator placed in a dark place.

Preparation of Polymer Solutions. Polymer solutions of various concentrations were prepared by mixing by weight the solvent and a known concentration solution. They were freed from dust by centrifugation. An antioxidant, about 0.05 w/v % 2,6-di-*tert*-butyl-*p*-cresol, was added in the solutions because antioxidant-free solutions showed oxidative degradation during the measurements for a long time, say, 1 h. All the preparative procedures were proceeded in dryboxes under N_2 atmosphere above 32 °C. The solutions thus prepared were stored, under the shade of light, in a box, its temperature being kept above 32 °C.

Dynamic Light Scattering. The intensity autocorrelation function $A(\tau)$ was measured at 34.7 ± 0.02 °C by the same apparatus and procedures described earlier.[6] A vertically polarized single-frequency 488-nm line of argon-ion laser fitted with a space etalon was used as the light source. The scattering angle was fixed at four positions, i.e., 30°, 60°, 90°, and 120°.

Results and Discussion

Method of Data Analysis. At the scattering angles θ = 30° and 60° for L-14, θ = 30° for L-12, and θ = 30° for L-11, the quantity X ($\equiv q^2 R_G^2$) was in the range from 0.03 to 0.24. Here q is the magnitude of the scattering vector. The translational diffusion coefficients at finite polymer concentration $D(c)$ for the above three samples were estimated by fitting the $A(\tau)$ data to a single exponential curve of the decay rate or the first cumulant $\Gamma(c)$ ($\equiv D(c)q^2$); i.e., $A(\tau) = \beta \exp(-2\Gamma(c)\tau) + 1 + \delta$. Here β is a fitting parameter representing the amplitude and δ is a fitting deviation of the base line from 1.000. The values of δ were ±0.003. This confirmed the high reliability of present $A(\tau)$ data and the analyses. Figure 2 shows the $D(c)$ plotted against the concentration c. For each sample, the $D(c)$'s are well represented by the straight line, and the infinite dilution value D_0 and the concentration coefficient k_D were determined from

$$D(c) = D_0(1 + k_D c) \qquad (2)$$

The results are summarized in Table II.

At θ = 120° for L-12 and at θ = 60°, 90°, and 120° for L-11, X ranged from 0.6 to 2.7. Hence, the $A(\tau)$ data were analyzed by the histogram method[10] of bimodal distribution $G(\Gamma)$, of which the first (slow) mode was assigned to the translational diffusion motion. The effective decay rate (the first cumulant) at finite q and c, $\Gamma_e(q,c)$ was estimated by averaging Γ over the distribution $G(\Gamma)$. The amplitude of the translational diffusion mode relative to all molecular motions P_0/P was also evaluated from the fractional area of the first component in $G(\Gamma)$. Figure 3 shows concentration dependences of $\Gamma_e(q,c)/\sin^2(\theta/2)$ at constant q for solutions of L-11 and L-12. The data for given q are represented well by a straight line and give the value at infinite dilution, $\Gamma_e(q,0)$. These values are listed in Table III. The negative slopes in Figure 3 are characteristic of Γ_e in Θ-solvents.[3] Figure 4 shows concentration depen-

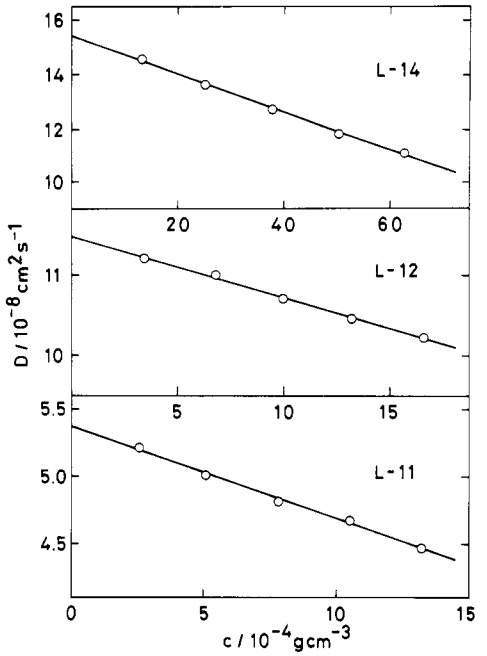

Figure 2. Concentration dependence of the translational diffusion coefficient D obtained for three PIP samples in 1,4-dioxane at 34.7 °C.

Table II
Results of Dynamic Characteristics D_0, R_H, k_D, and ρ Obtained for Polyisoprenes in 1,4-Dioxane at 34.7 °C

polymer	D_0, 10^{-8} cm^2 s^{-1}	R_H, 10^{-6} cm	k_D, cm^3 g^{-1}	ρ
L-14	15.4_2	1.43_5	−45.3	1.33
L-12	11.4_8	1.92_7	−66.2	1.31
L-11	5.37_4	4.11_7	−128	1.27

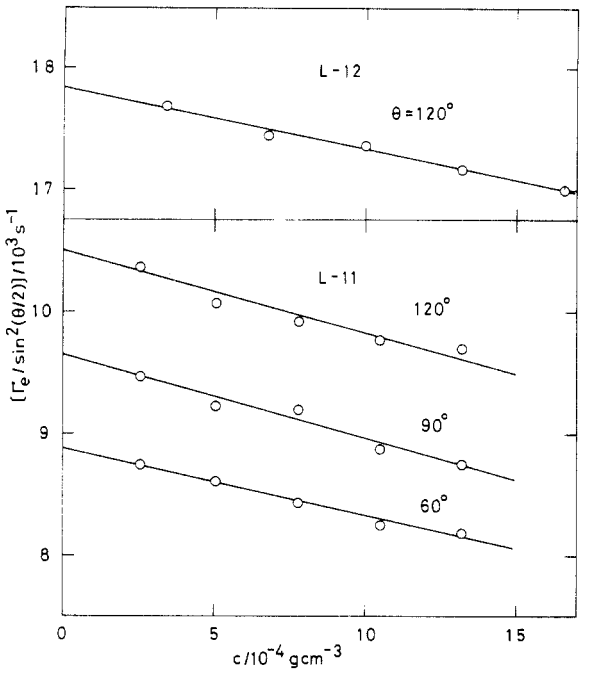

Figure 3. Linear extrapolation of the reduced effective decay rates $\Gamma_e(q,c)/\sin^2(\theta/2)$ for the solutions of L-12 at the scattering angle θ = 120° and L-11 at θ = 60°, 90°, and 120°.

Table III
Results of Effective Decay Rate (First Cumulant) and Relative Amplitude of Translational Diffusion Motion at Infinite Dilution, $\Gamma_e(q,0)$ and $(P_0/P)_{c\to 0}$, Obtained for Polyisoprenes in 1,4-Dioxane at 34.7 °C

polymer	angle, deg	X	$\Gamma_e(q,0)/q^2$, 10^{-8} s^{-1}	$(P_0/P)_{c\to 0}$
L-11	120	2.74_2	7.86_0	0.845
	90	1.82_8	7.23_4	0.912
	60	0.914_0	6.64_6	0.965
	30	0.244_9	5.37_6	
	$\theta \to 0$	0.0	5.37_6	
L-12	120	0.636_6	13.35	0.985
	30	0.0569	11.49	
	$\theta \to 0$	0.0	11.49	
L-14	60	0.121_9	15.42	
	30	0.0327		
	$\theta \to 0$	0.0	15.42	

dences of P_0/P at constant q for L-11 and L-12. The values of P_0/P at given q are nearly independent of c, as was the case for PS at the Θ-temperature,[3] and give the infinite dilution values $(P_0/P)_{c\to 0}$ within experimental error of 4%. The results are also summarized in Table III.

Translational Diffusion Coefficient. The molecular weight dependence of translational diffusion coefficients (D_0) listed in Table II can be given by

$$D_0 = 8.68 \times 10^{-5} M_w^{-0.50\pm0.02} \tag{3}$$

The D_0 values were converted to the equivalent hydrodynamic radius (R_H) by the relation

$$D_0 = k_B T/6\pi\eta_0 R_H \tag{4}$$

where k_B is Boltzmann's constant and T is the absolute temperature. These values of R_H versus M_w are represented in Figure 1 by the filled circles. They are well represented by

$$R_H = 2.57 \times 10^{-9} M_w^{0.50\pm0.02} \quad \text{(cm)} \tag{5}$$

The exponent of M_w, 0.50±0.02, though its uncertainty is a little bit large due to three data points fitting, assures us that the present polymer–solvent system is in the Θ-state. Since the R_G data give the relation $R_G \propto M_w^{0.50}$, as

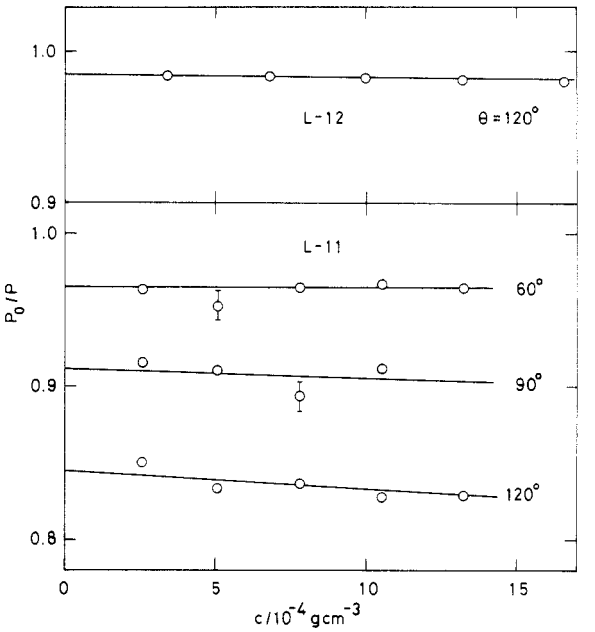

Figure 4. Linear extrapolation of the amplitude of the translational diffusion motion relative to the total motion P_0/P for the solutions of L-12 at θ = 120° and L-11 at θ = 60°, 90°, and 120°.

already shown in the same figure by unfilled symbols, it is found that both R_H and R_G have the same M_w dependence and R_H is smaller than R_G over the entire molecular weight region investigated.

Defining a dimensionless parameter ρ by

$$\rho \equiv R_G/R_H \tag{6}$$

we can estimate its value as listed in Table II. The ρ was 1.30 ± 0.03, independent of the molecular weight. This value agrees, to within experimental error, with 1.27–1.28[3] for PS in Θ-solvents. It is thus found that the value is unaffected by the chain flexibility. However, this value of ρ is by about 13% smaller than 1.504 (=ρ_K) or 1.479 predicted by the classical theories of Kirkwood[11,12] or Zimm[13] with preaveraged and/or nonpreaveraged Oseen hydrodynamic interaction. We note also that the present value of 1.30 lies in the middle of 1.40 ± 0.01,[14] calculated by a Monte Carlo simulation, and 1.190,[15] calculated from the renormalization-group techniques under non-PA scheme. Still another value of ρ, 1.285, has recently been obtained by Zimm[16] based on the simulation for Gaussian and cubic lattice chains. According to Fixman,[17] Zimm's algorithm gives a "lower-bound" value, ρ_{LB}, which is attained in a rigid body motion at sufficiently strong internal friction. Fixman[17] has revealed the following: (1) if the friction constants are independent of local chain structure, an "upper-bound" value, ρ_{UB}, stays at about 1.38 (8% below ρ_K) irrespective of long Gaussian chains or lattice chains; (2) however, the ρ_{UB} decreases down to near ρ_{LB} when a very small amount of *internal friction* is introduced, which depends on the specified local nature of the chains.

In this connection, it may be interesting to note that in good solvent system, ρ_{good} was about 1.5 for both PIP and PS and that the ratio to the Θ-value ρ_{good}/ρ_Θ = 1.15 was close to 1.06 or 1.08, which was obtained by combining Kirkwood's[11,12] or Zimm's[13] ρ_Θ with ρ_{good} for the Domb–Gillis–Wilmers segment distribution.[6,18]

Internal Motions. Figure 5 shows, by the unfilled circles with vertical pip, the X dependence of the reduced value $\Gamma_e(q,0)/D_0q^2$ for the present data of PIP in 1,4-dioxane. The other circles are our previous data: the unfilled ones for PIP in cyclohexane (good solvent) at 25 °C[6] and

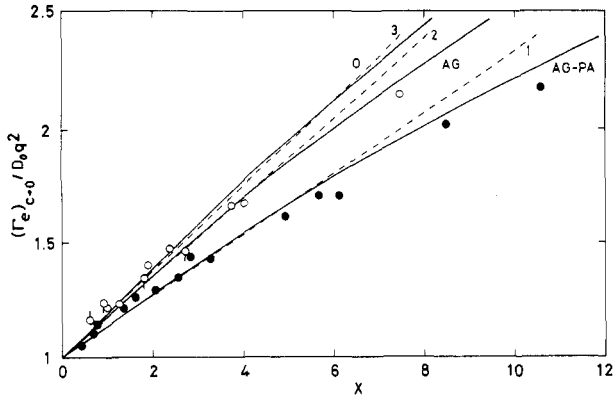

Figure 5. Plots of the reduced values of $\Gamma_e(q,0)/D_0q^2$ against $X(=q^2R_G^2)$: (♀) L-11 and (♁) L-12, the present data for PIP in 1,4-dioxane at 34.7 °C; (O) PIP data in cyclohexane at 25 °C[6]; (●) PS data in *trans*-decalin at 20.4 °C.[3] The solid curves are the theoretical curves calculated for nondraining Gaussian chains: (AG–PA) Akcasu–Gural[19-21] curve with PA Oseen hydrodynamics; (AG) A–G curve with non-PA; (O) Oono[22] curve with non-PA. The broken lines represent the initial slopes for each curve: (1) 2/15; (2) 13/75; (3) 0.187.

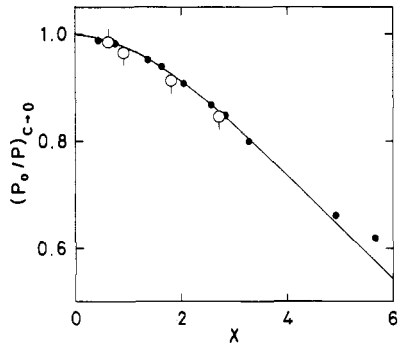

Figure 6. X dependence of the relative amplitude of translational diffusion motion $(P_0/P)_{c\to 0}$: (♀) L-11 and (♁) L-12 for the PIP data in 1,4-dioxane at 34.7 °C; (●) PS data in *trans*-decalin at 20.4 °C.[3] The solid curve represents the theoretical value for nondraining Gaussian chains.

the filled ones for PS in *trans*-decalin at Θ-temperature.[3] The solid curves AG and O are the theoretical curves of Akcasu–Gurol (A–G)[19-21] and Oono,[22] respectively, for the nondraining Gaussian chains with non-PA Oseen hydrodynamics, and the curve AG–PA is the A–G curve with PA hydrodynamics. The broken lines 1, 2, and 3 represent the initial slopes, 2/15, 13/75, and 0.187, for curves AG–PA, AG, and O, respectively. The PIP data are located near curve AG and support non-PA hydrodynamics irrespective of the solvent power. This is different from the PS data; they are located near curve AG–PA. The difference might be attributed to the high chain flexibility of PIP chains.

Figure 6 shows the amplitude of the translational diffusion motion relative to the total motion, $(P_0/P)_{c\to 0}$, as a function of X. Here the unfilled circles represent the PIP data, the filled circles our previous data for PS at Θ-temperature,[3] and the solid curve the theoretical one for *nondraining* Gaussian chains.[10] The data fall well on the curve and reconfirm the adequacy of the nondraining model.

Intermediate-Scale Motions. In Figure 7, the reduced effective decay rate $\Gamma_e(q,0)/(q^3k_BT/\eta_0)$ is plotted against $X^{1/2}$ for PIP (unfilled circles) and for PS (filled circles). The solid curves AG–PA, AG, and O represent the theoretical curves with the same meanings as in Figure 5 and give the asymptotic values at the large region of $X^{1/2}$; 0.053 (AG–PA), 0.0625 (AG), and ca. 0.027 (O), respectively. Since the PIP data do not extend to a wide range of $X^{1/2}$,

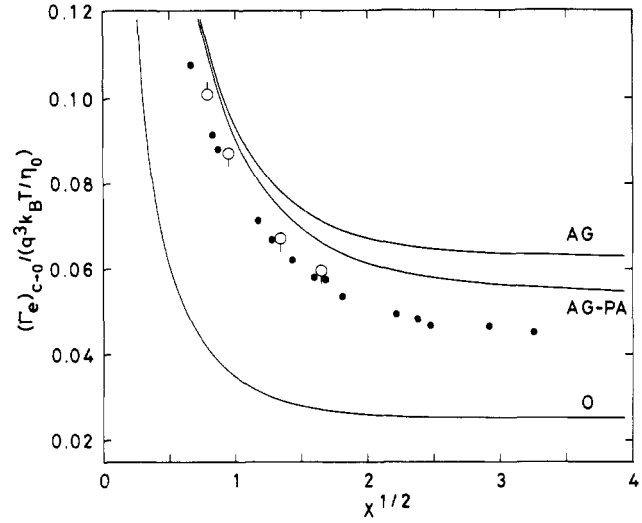

Figure 7. Plots of the reduced effective decay rate $\Gamma_e(q,0)/(q^3k_BT/\eta_0)$ against $X^{1/2}$: (♀) L-11 and (♁) L-12 for the PIP data in 1,4-dioxane at 34.7 °C; (●) PS data in *trans*-decalin at 20.4 °C. The solid curves are the theoretical curves calculated for nondraining Gaussian chains; (AG–PA) A–G curve[19-21] with PA; (AG) A–G with non-PA; (O) Oono[22] curve with non-PA.

they show no asymptotic feature as yet. However, they are located above and nearly parallel to the PS data within the range of $X^{1/2}$ measured. This situation might give us an appropriate symptotic value 0.048 for PIP, while PS has given 0.045 at large X.[3] Since the PIP data are well represented by non-PA calculation as mentioned in the previous section, we compare the result with the non-PA curve. The value 0.048 for PIP is however still smaller than the curve AG by 20%. At present there is no explanation as to why the difference is so large in the Θ-state. As referred in D_0, it may be expected that the *internal friction* would influence the $\Gamma_e(q,0)$ value. Stockmayer and Hammouda[4] have recently found some reduction of Γ_e by advancing this scheme, but no reliable numerical estimate has been available.

Concentration Dependence of Translational Diffusion Coefficient. At the Θ-temperature, the coefficient k_D is related directly to the coefficient k_f of the concentration dependence of the fraction coefficient as[23,24]

$$k_D = -(k_f + \bar{v}) \tag{7}$$

where $\bar{v}$ is the partial specific volume of the polymer, and $\bar{v} \approx 1.1$ cm^3 g^{-1} for PIP. For k_f, several theories have been derived. They are summarized in the form

$$k_f = BN_AV_H/M_w = B'M_w^{1/2} \tag{8}$$

where N_A is Avogadro's number and V_H the hydrodynamic volume defined by $V_H = (4\pi/3)R_H^3$. In the large region of M_w, the coefficient k_D becomes proportional to $M_w^{1/2}$ because $\bar{v}$ ($\approx$1.1) is negligibly small.[24] Theoretically the magnitude of B in eq 8 is 1.0 for the bead-spring model of Yamakawa[23] and Imai[25] (YI) and 2.23 for the soft-equivalent-sphere model of Pyun and Fixman[26] (PF) (Figure 8). Mulderije[27] has revised the PF value as 2.06 (M) and also shown, based on the study of Batchelor,[28] that B = 1.60 (MBa). Akcasu[29] has proposed another value B = 1.29 (A) by using three different models for the intermolecular interactions. It is noted that the origin of B = 1.0 by YI and the other values of B from other theories are different in the physical mechanisms they represent.[36]

The data of k_D, listed in Table II, give the molecular weight dependence:

$$k_D = -8.30 \times 10^{-2}M_w^{0.50\pm0.05} \quad (\text{cm}^3\ \text{g}^{-1}) \tag{9}$$

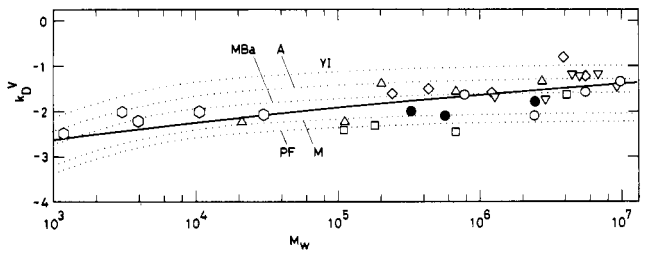

Figure 8. Plots of volume-fraction coefficient k_D^V against M_w for the present data of PIP in 1,4-dioxane at 34.7 °C (●). The unfilled symbols are the data for PS in cyclohexane at 35 °C: (△) King et al.;[31] (□) Han;[32] (▽) Jones and Caroline;[33] (◇) Varma et al.;[34] (○) Huber et al.[35] and in *trans*-decalin at 20.4 °C: (○) Tsunashima et al.[3] The dotted curves are the theoretical curves with the following B in eq 8: (YI) $B = 1.0$;[23,25] (A) 1.29;[29] (MBa) 1.60;[27,28] (M) 2.06;[27] (PF) 2.23.[26] The solid curve represents the best fit value for PS obtained by Tsunashima et al.:[30] $k_D = -0.13M_w^{0.43}$ cm^3 g^{-1}.

The exponent 0.50 confirms eq 8, the theoretical prediction at Θ-temperature. This is in contrast to the results for PS in Θ-solvents, where the best-fit exponent to all the data available was 0.43 ± 0.02.[30] For convenience' sake, the measured k_D of mass fraction coefficient can be transformed into the volume fraction one, k_D^V, through a relation $k_D^V = k_D M_w/N_A V_H$. Figure 8 shows the M_w dependence of the k_D^V for PIP (filled circles). Here V_H was calculated from R_H in Table II. The dotted curves YI, A, MBa, M, and PF represent the theoretical curves with B mentioned above. They show strong curvatures in the low M_w region due to the large contribution of $\bar{v}$ to k_D^V. The PIP data are located nearly on curve M ($B = 2.06$) rather than curve YI. This is in contrast to the results in good solvents where the Yamakawa theory was adequate.[6] By unfilled symbols in the figure, we also show the molecular weight dependence of k_D^V values reported hitherto for PS in Θ-solvents (*trans*-decalin and cyclohexane).[31-35] The values of V_H were calculated from experimental values of R_H reported in the references concerned. The correction of $\bar{v}$ was also made to k_D^V in low molecular weight region. These PS data are located roughly between curves YI ($B = 1.0$) and PF ($B = 2.23$); in the region $M_w > 2 \times 10^5$, they are closer to curve MBa ($B = 1.60$), while in the lower M_w region, $M_w < 3 \times 10^4$, they lie between curves A ($B = 1.29$) and M.[37] On the whole, all the data ranging from $M_w \approx 10^3$ to 10^7 are satisfactorily represented by the solid curve which was transformed from the mass fraction k_D versus M relation

$$k_D = -0.13M_w^{0.43} \quad (\text{cm}^3\ \text{g}^{-1}) \tag{10}$$

with use of $R_H = 2.29 \times 10^{-9} M_w^{0.50}$ cm for PS in cyclohexane at 35 °C.[1] Equation 10 has been reported previously by us as the best fit curve for PS.[30]

Conclusions

The PIP chains in 1,4-dioxane at 34.7 °C were found to be adequate to study dynamical properties of linear flexible chains in the unperturbed state. The dynamic properties were well described by the *nondraining* chain model with *nonpreaveraged* Oseen hydrodynamic interaction. However, there still remains some differences between experiments and theories in the magnitude of D_0 (or ρ) and $\Gamma_e(q,0)$.

Registry No. PIP, 9003-31-0; 1,4-dioxane, 123-91-1.

References and Notes

(1) Schmidt, M.; Burchard, W. *Macromolecules* **1981**, *14*, 210.
(2) Han, C. C.; Akcasu, A. Z. *Macromolecules* **1981**, *14*, 1080.
(3) Tsunashima, Y.; Nemoto, N.; Kurata, M. *Macromolecules* **1983**, *16*, 1184.
(4) Stockmayer, W. H.; Hammouda, B. *Pure Appl. Chem.* **1984**, *56*, 1373.
(5) Nemoto, N.; Makita, Y.; Tsunashima, Y.; Kurata, M. *Macromolecules* **1984**, *17*, 425.
(6) Tsunashima, Y.; Hirata, M.; Nemoto, N.; Kurata, M. *Macromolecules* **1987**, *20*, 1992.
(7) Hadjichristidis, N.; Roovers, J. E. L. *J. Polym. Sci., Polym. Phys. Ed.* **1974**, *12*, 2521.
(8) Riddick, J. A.; Bunger, W. B. *Organic Solvents*, 3rd ed.; Wiley-Interscience: New York, 1970.
(9) Hirata, M. Masters Thesis, Kyoto University, 1986. The detailed discussion will be made in a forthcoming paper.
(10) Tsunashima, Y.; Nemoto, N.; Kurata, M. *Macromolecules* **1983**, *16*, 584.
(11) (a) Kirkwood, J. G.; Riseman, J. *J. Chem. Phys.* **1948**, *16*, 565. (b) Kirkwood, J. G. *J. Polym. Sci.* **1954**, *12*, 1.
(12) Benmouna, M.; Akcasu, A. Z. *Macromolecules* **1978**, *11*, 1187.
(13) Zimm, B. H. *J. Chem. Phys.* **1956**, *24*, 269.
(14) Guttman, C. M.; McCrackin, F. L.; Han, C. C. *Macromolecules* **1982**, *15*, 1205.
(15) Oono, Y.; Kohmoto, M. *J. Chem. Phys.* **1983**, *78*, 520. The ρ value was revised since simple mathematical errors were found in the article.
(16) Zimm, B. H. *Macromolecules* **1980**, *13*, 592.
(17) Fixman, M. *J. Chem. Phys.* **1986**, *84*, 4080, 4085.
(18) Tsunashima, Y.; Kurata, M. *J. Chem. Phys.* **1986**, *84*, 6432.
(19) Akcasu, A. Z.; Gurol, H. *J. Polym. Sci., Polym. Phys. Ed.* **1976**, *14*, 1.
(20) Burchard, W.; Schmidt, M.; Stockmayer, W. H. *Macromolecules* **1980**, *13*, 580.
(21) Akcasu, A. Z.; Benmouna, M.; Han, C. C. *Polymer* **1980**, *21*, 866.
(22) Oono, Y. *Adv. Chem. Phys. Prepr.* **1987**, *1*. The value ρ was revised by us.
(23) Yamakawa, H. *Modern Theory of Polymer Solutions*; Harper and Row: New York, 1971.
(24) According to Kops-Werkhoven et al. (Kops-Werkhoven, M. M.; Vrij, A.; Lekkerkerker, H. N. W. *J. Chem. Phys.* **1983**, *78*, 2760), the term $\bar{v}$ should be omitted. This affects strongly the values of k_D^V in the small M_w region such as $M_w < 10^4$ (see Figure 8).
(25) Imai, S. *J. Chem. Phys.* **1970**, *52*, 4212.
(26) Pyun, C. W.; Fixman, M. *J. Chem. Phys.* **1964**, *41*, 937.
(27) Mulderije, J. J. H. *Macromolecules* **1980**, *13*, 1207, 1526.
(28) Batchelor, G. K. *J. Fluid Mech.* **1972**, *52*, 245.
(29) Akcasu, A. Z. *Polymer* **1981**, *22*, 1169. It should be noticed that B depends on the models used sensitively and that any value between 1.0 (Y) and 2.23 (PF) can be obtained by adjusting some parameters in the models.
(30) Tsunashima, Y.; Nemoto, N. *Macromolecules* **1983**, *16*, 1941.
(31) King, T. A.; Knox, A.; Lee, W. I.; McAdam, J. D. G. *Polymer* **1973**, *14*, 151.
(32) Han, C. C. *Polymer* **1979**, *20*, 259.
(33) Jones, G.; Caroline, D. *Chem. Phys.* **1979**, *37*, 187.
(34) Varma, B. K.; Fujita, Y.; Takahashi, M.; Nose, T. *J. Polym. Sci., Polym. Phys. Ed.* **1984**, *22*, 1781.
(35) Huber, K.; Bantle, S.; Lutz, P.; Burchard, W. *Macromolecules* **1985**, *18*, 1461.
(36) For further discussion, Jamieson's paper (Bull. *Am. Phys. Soc.* **1987**, *32*, 3) should be referenced.
(37) For PS in cyclohexane at 34.5 °C, ref 35 showed that R_H deviated from the power law $R_H \propto M^{0.5}$ at $M_W < 3 \times 10^4$, and Huber and Stockmayer[38] have also shown that A_2 was larger than zero at $M_w < 10^4$. The discussion on k_D^V is thus left open for very low M_w as $M_w < 3 \times 10^4$.
(38) Huber, K.; Stockmayer, W. H. *Macromolecules* **1987**, *20*, 1400.